



Efficient conversion of leather tanning waste to biodiesel using crab shell-based catalyst: WASTE-TO-ENERGY approach

Maria Yuliana^{a,*}, Shella Permatasari Santoso^{a,b}, Felycia Edi Soetaredjo^{a,b}, Suryadi Ismadji^{a,b}, Aning Ayucitra^a, Chintya Gunarto^b, Artik Elisa Angkawijaya^c, Yi-Hsu Ju^{b,c,d}, Chi-Thanh Truong^e

^a Department of Chemical Engineering, Widya Mandala Catholic University Surabaya, Kalijudan 37, Surabaya, 60114, Indonesia

^b Department of Chemical Engineering, National Taiwan University of Science and Technology, 43, Keelung Rd. Sec. 4, Taipei, 10607, Taiwan

^c Graduate Institute of Applied Science and Technology, National Taiwan University of Science and Technology, 43 Keelung Road, Sec 4, Taipei, 10607, Taiwan

^d Taiwan Building Technology Center, National Taiwan University of Science and Technology, 43 Keelung Road, Sec 4, Taipei, 10607, Taiwan

^e Department of Chemical Engineering, Can Tho University, 3-2 Street, Can Tho City, Viet Nam

ARTICLE INFO

Keywords:

Leather tannery waste
Crab shell
Biodiesel
Waste-derived fuel
Reusability
Optimization study

ABSTRACT

To promote the use of waste-originated resources in biodiesel production, this study proposes the utilization of leather tanning waste (LTW) and crab-shell (CS) waste as the respective lipid source and catalyst material. The obtained CS-based calcium oxide (CaO) has comparable textural properties with those of existing waste-based catalysts and shows high catalytic activity for the conversion of LTW to biodiesel. The optimum yield of fatty acid ethyl esters (FAEE) is predicted at 97.9 wt%, while it is experimentally observed at 98.7 ± 0.4 wt% (purity of 98.6 ± 0.4 wt%) using the following operating condition: reaction time $t = 3.58$ h, catalyst amount $m_c = 3.87$ wt%, and a molar ratio of ethanol to LTW $m_{eo} = 12:1$. The CS-based CaO shows good reusability with FAEE yield staying above 90 wt% for four cycles. The fuel properties of LTW-based biodiesel meet ASTM D6751 and ASTM D975-08 standards, with the ethyl ester ranging from C14 to C20.

1. Introduction

Worldwide interest in the use of waste to fulfill the energy demand is currently growing in a very rapid manner. Many types of research related to waste-to-energy have been conducted to improve the transesterification yield, find the simplest and low-cost technique as well as fabricate waste-based catalysts. Known as an archipelago country, the aquaculture industries are one of the biggest and most important sectors in Indonesia. Approximately 30,000 tons of crab are produced annually, where its meat only accounts for only around 35 wt% of the total crab mass. This leaves almost 20,000 tons of solid waste discharged each year [1]. While in the developed countries, waste disposal is costly, crab shells (CS) in Indonesia are often directly discharged to the environment.

CS exhibits potential value due to its valuable chemical contents, namely protein (20–40 wt%), calcium carbonate (20–50 wt%), and

chitin (15–40 wt%) [2]. Being the largest component in CS, calcium carbonate finds extensive applications in pharmaceutical, agricultural, material development, and catalysis. Many studies have been conducted to develop calcium-based solid catalyst, with calcium oxide (CaO) as the main focus due to its advantages of substantial catalytic activity, high basicity, non-toxicity [3,4], good availability, and low cost [5]. In addition, the conversion of calcium carbonate to CaO can be achieved using a relatively simple method, that is, by thermal decomposition via calcination at high temperatures to liberate carbon dioxide from the raw materials [6].

Currently, transesterification of lipid to biodiesel is employed mainly using a homogenous catalyst, due to its phase homogeneity and shorter reaction time [5,7]. However, this type of catalyst cannot be reused and requires additional washing and separation steps, hence inducing attention in the use of the heterogeneous solid catalyst for the biodiesel preparation process. Despite its comparable catalytic activity and

Abbreviations: ANOVA, Analysis of variance; CaO, Calcium oxide; CS, Crab shell; DOE, Design of experiment; FA, Fatty acid; FAEE, Fatty acid ethyl esters; FFA, Free fatty acid; FID, Flame ionized detection; LTW, Leather tanning waste; MLFD, Multilevel factorial design; RSM, Response surface methodology; SEE, Standard error of estimate; TGA, Thermogravimetric analysis.

* Corresponding author.

E-mail addresses: maria_yuliana_liauw@yahoo.com, mariayuliana@ukwms.ac.id (M. Yuliana).

<https://doi.org/10.1016/j.biombioe.2021.106155>

Received 8 January 2021; Received in revised form 16 May 2021; Accepted 6 June 2021

0961-9534/© 2021 Elsevier Ltd. All rights reserved.

simpler use in the transesterification process, many heterogeneous catalysts are not viable for industrial usage since most of the catalysts are expensive and require complicated preparation efforts [8,9]. Therefore, synthesizing simple yet highly active catalysts for biodiesel preparation is important. Due to this very reason, an increasing number of studies on the neat, supported, loaded, and mixed CaO has been widely investigated [3,6]. The high catalytic activity of CaO might be attributed to the presence of oxygen attached to its surface, which acts as a strong basic conjugate [10]. These basic sites abstract a proton from the organic compounds and initiate the basic catalysis reaction [6]. The catalytic activity of CaO-based catalyst in the transesterification has been conducted using various natural-based raw materials as follows: mussel shells [11,12], eggshells [13], waste capiz shells [8,9], cockle shells [12], Pomacea sp. shells [14] and river snail shells [15]. Extensive utilization of waste-based catalysts is expected to reduce the material cost as well as to conduct a good waste management practice.

To date, the development of waste-based solid catalyst mainly focuses on the conversion of refined oils, rather than waste lipid materials, to biodiesel. The selection of refined oils as the raw materials is generally due to its low free fatty acid (FFA) and moisture content; therefore, it is easier to process and gives a more stable yield. However, the mass utilization of this type of lipid will disrupt the food supply chain. Yuliana et al. [16] mentioned that non-edible oils, specifically fat, oil, and grease (FOG) and animal fats, are currently the best options for biodiesel feedstock compared to edible ones due to their low price. Moreover, the valorization of the waste-based lipid will significantly lessen the amount of the waste, and at the same time, turn them into a valuable asset. Therefore, this study combines the use of CS-based catalysts and leather tanning waste (LTW) as a lipid source to produce biodiesel.

With 80 wt% of the rawhide is discharged as waste during the commercial tanning process of leather [17,18], the annual production of LTW in Indonesia reaches 100,000 tons [19,20]. LTW contains a substantial amount of crude fat (>60 wt%) [18] that can be converted to biodiesel; which renders it an abundant raw material to prepare biodiesel. A number of valorization approaches have been previously conducted to prepare biodiesel from LTW, namely using supercritical methanol [20], Cs₂O-loaded Fe₃O₄ nanoparticles [21], solid-state fermentation using silica-immobilized micro bacteria soaked in inorganic nutrients (e.g., MgSO₄, FeSO₄, CoCl₂, MnCl₂, CaCl₂, and (NH₄)₆Mo₇O₂₄) [22], and conventional basic catalyst (e.g., potassium methoxide [23], sodium and potassium hydroxide [24,25], and methanolic tetramethylammonium hydroxide [26]). While the first three techniques require a high amount of energy and complicated processing steps, the last technique using basic catalysts often faces many challenges due to the presence of high water and FFA content. These two components promote the hydrolysis and saponification reactions during the traditional conversion [16], which leads to a difficult separation and lower yield. Therefore, with the above-mentioned advantages of simple preparation, low cost, and insensitivity to contaminants during use, CS-based CaO can be considered highly potential to prepare biodiesel with commercial yield and specification from LTW in one-pot transesterification. Besides, due to the nature of the two waste materials, a waste-to-energy approach can be achieved via the utilization of CS and LTW as the starting catalyst and biodiesel feedstocks, respectively.

The influence of three independent processing variables (catalyst loading m_c , reaction time t , and the molar ratio of ethanol to LTW m_{eo}) on the yield of fatty acid ethyl esters (FAEE) is studied. The optimization approach is conducted using a combination of response surface methodology (RSM) and multilevel factorial design (MLFD) to obtain the optimized reaction parameters, which can be implemented in industrial practice. Among many statistical and mathematical approaches, MLFD

is selected because it (1) incorporates all interactions of the three variables at all levels, and (2) offers more flexibility in assessing these interactions when the number of degrees of freedom is sufficient [27]. Moreover, the use of the factorial design also increases the statistical sensitivity and generalizability without decreasing precision [28]; therefore, it is superior compared to the other methods. This study also uses ethanol as the alcohol source to maintain the phase homogeneity in the reaction system which leads to an increase in reaction rate [29,30]. The reusability of the CS-based CaO is also monitored at the optimum operating condition.

2. Materials and methods

2.1. Materials

Both raw waste materials, CS and LTW, were collected from a local supplier in Surabaya, Indonesia. While CS was obtained from a local fish market, LTW was provided by a leather tannery in Indonesia. The pre-treatment of CS was conducted using the following procedures [8]: CS was first rinsed to remove the impurities. The cleansed CS was pulverized to a powder and subjected to the calcination process at 900 °C for 2 h. The calcined CS was further ground to a powder with a particle size of smaller than 25 µm. The obtained powder was then stored in a vacuum container before use. At the same time, LTW was washed with water to remove unwanted dirt and impurities, followed by heating at 120 °C to remove retaining moisture. LTW was then purified using a membrane filter.

All solvents and chemicals used for biodiesel preparation and analysis were purchased from Merck (Germany) and of analytical grade; therefore, does not require any further purification. The gases required for gas chromatography analysis, namely nitrogen and helium (>99.9%) were procured from Aneka Gas Industry Pty. Ltd., Surabaya. The composition of the biodiesel product was identified using the FAEE certified reference (10008188) obtained from Cayman Chemicals (MI, USA), while methyl heptadecanoate, which acts as the internal standard to calculate the purity of FAEE, was purchased from Sigma-Aldrich (Germany).

2.2. The properties determination of CS-based CaO and LTW

The surface topography and morphology images of CS-based CaO were captured by FESEM JEOL JSM-6500F (Jeol Ltd., Japan), with the respective voltage and working distance of 10 kV and 8.0 mm. Meanwhile, the textural properties of CS-based CaO, such as its specific surface area and pore volume, were obtained using Micromeritics ASAP 2010 Sorption Analyzer at 77 K. The XRD diffractogram of the catalyst was acquired in $2\theta = 15^\circ\text{--}90^\circ$ using an X'PERT Panalytical Pro X-Ray diffractometer (Philips-FEI, Netherlands). The wavelength of monochromatic Cu K α_1 radiation (λ) is set at 0.154 nm. The voltage and tube current is adjusted at 40 kV and 30 mA, respectively. To measure its thermal stability, 6 mg of CS-based CaO powder were placed in a platinum pan and subjected to a PerkinElmer TG/DTA Diamond (PerkinElmer, Japan). The oven temperature was then increased from 30 °C to 900 °C at a rate of 10 °C/min under a continuous nitrogen purge (velocity of nitrogen purge = 20 ml/min) to monitor the degradation profile of the CS-based CaO.

Meanwhile, the crude fat, FFA, and moisture content in LTW were determined following AOAC 991.36, ASTM D5555-95, and AOCs Ca 2e-84, respectively. LTW is also further analyzed for its fatty acid (FA) profile using GC-2014 (Shimadzu Ltd., Japan), following the method of ISO 12966. Restek Rtx-65TG (30 m × 0.25 mm ID × 0.10 µm film

Table 1
The encoded reaction parameters and their corresponding values.

Variables	Encoded factor	Factor level				
		1	2	3	4	5
Catalyst loading (mc, wt%)	A	1	2	3	4	5
		1	2	3		
Reaction time (t, h)	B	2	3	4		
Molar ratio of ethanol to LTW (m_{eo})	C	6:1	9:1	12:1		

thickness, Restek, USA) was selected as the separation column to identify the FA profile in LTW.

2.3. Biodiesel preparation using LTW and CS-based CaO

Ethanol as the alcohol source and LTW at $m_{eo} = 6:1, 9:1, \text{ and } 12:1$ was added into a three-neck flask, fully installed along with a condenser, magnetic stirrer, and heater. A specified amount of CS-based CaO ($m_c = 1, 2, 3, 4, 5 \text{ wt\%}$) was introduced into the system. The reaction system was then heated to $60 \text{ }^\circ\text{C}$ and maintained isothermally throughout the process with constant agitation at 700 rpm for various t (2, 3, 4 h). After the reaction was completed, the catalyst was separated from the liquid product mixture by centrifugation and regenerated through a cycle of repeated washing and calcination at $900 \text{ }^\circ\text{C}$. The product mixture was settled to obtain two layers, the top layer consisting FAEE and other minor components, and the bottom layer which is the mixture of glycerol, excess ethanol, and other undesirable by-products. The separated FAEE-rich phase was then subjected to vacuum evaporation to obtain the biodiesel product.

Using the optimized reaction condition obtained in section 2.5, a repetition of transesterification using the same catalyst was performed until the yield of FAEE reached below 90 wt\% to measure the reusability of the CS-based CaO. All runs were conducted in triplicates.

2.4. Compositional analysis of LTW-based biodiesel using GC-FID

The FAEEs composition in the LTW-based biodiesel was identified by Shimadzu GC-2014, with the split/splitless injection and the flame ionized detection (FID) mode. The stationary silica phase used in the chromatography separation is the narrow bore type of DB-WAX capillary column ($30 \text{ m} \times 0.25 \text{ mm ID} \times 0.25 \text{ } \mu\text{m}$ film thickness, Agilent Technology, CA). Before analysis, 100 mg of biodiesel product was dissolved in 2 ml of methyl heptadecanoate solution ($10 \text{ } \mu\text{g/ml}$) which acts as an internal standard. The mixture was then injected at a split ratio of 1:50 into the GC column which temperature has been initially adjusted at $50 \text{ }^\circ\text{C}$ before injection. The temperature profile of the instrument and the carrier gas (helium, $> 99.9\%$) purge flowrate for the compositional analysis follows the study performed by Santosa et al. [31].

The chromatogram of the FAEE certified reference (10008188) was used against that of the biodiesel product to identify the FAEE peaks. The FAEE purity and yield were computed using equations (1) and (2).

$$FAEE \text{ Purity } (F_p, \text{ wt\%}) = \left(\frac{\sum A_{FAEE} - A_{IS}}{A_{IS}} \times \frac{V_{IS} C_{IS}}{m_{FAEE}} \right) \times 100\% \quad (1)$$

where $\sum A_{FAEE}$ is the area sum of FAEE peaks, A_{IS} is the area of methyl heptadecanoate peak, V_{IS} is the volume of methyl heptadecanoate solution (ml), C_{IS} is the concentration of methyl heptadecanoate solution (g/ml), m is the actual mass of the FAEE sample used in the GC-FID analysis (g).

Table 2
The DOE matrix based on MLFD.

Run	Input variables			Response (FAEE yield, wt%)		
	A	B	C	Experimental ^a	Predicted (Y_{FAEE}) ^a	Standard deviation ^b
1	4	3	3	95.8	97.4	1.11
2	1	3	1	63.8	66.9	2.20
3	3	1	2	85.1	87.1	1.44
4	5	1	3	92.2	90.2	1.42
5	4	1	3	91.4	92.8	0.96
6	4	2	2	93.5	96.1	1.86
7	2	3	1	83.1	82.9	0.14
8	2	3	3	91.2	86.7	3.16
9	5	2	3	93.3	93.5	0.16
10	1	2	2	63.9	65.9	1.42
11	3	2	2	93.4	92.8	0.45
12	1	1	2	59.1	58.1	0.72
13	4	1	2	90.2	91.6	0.98
14	3	3	1	94.6	92.2	1.70
15	3	3	3	95.6	95.4	0.14
16	1	3	3	68.2	71.3	2.22
17	1	3	2	67.6	69.5	1.32
18	3	3	2	94.3	94.2	0.11
19	1	2	3	65.9	67.9	1.40
20	1	2	1	63.6	63.2	0.26
21	1	1	3	57.6	60.2	1.81
22	4	3	1	92.3	94.8	1.75
23	5	3	2	92.3	92.0	0.24
24	5	1	2	92.2	89.3	2.03
25	3	2	1	92.9	90.7	1.55
26	2	1	1	71.2	73.5	1.62
27	4	3	2	95.3	96.4	0.79
28	3	1	1	82.5	85.0	1.75
29	2	1	3	80.2	77.7	1.74
30	5	2	2	92.0	92.8	0.55
31	3	1	3	87.9	88.6	0.50
32	2	3	2	88.6	85.2	2.43
33	2	1	2	75.6	76.0	0.26
34	2	2	3	89.2	84.4	3.42
35	2	2	1	82.8	80.3	1.75
36	3	2	3	94.8	94.1	0.47
37	5	1	1	91.2	87.8	2.42
38	5	2	1	91.6	91.3	0.19
39	2	2	2	86.3	82.7	2.55
40	4	1	1	87.4	89.7	1.65
41	4	2	1	89.5	94.4	3.45
42	5	3	3	92.1	92.6	0.36
43	4	2	3	94.5	97.2	1.90
44	1	1	1	58.9	55.3	2.54
45	5	3	1	93.1	90.6	1.75

^a The average standard error of estimate (SEE) between the two corresponding responses is 1.24% .

^b The deviation between the two corresponding responses for each run.

$$FAEE \text{ Yield } (\text{wt\%}) = \left(\frac{m_{FAEE}}{m_{LTW}} \times F_p \right) \times 100\% \quad (2)$$

where m_{FAEE} is the final FAEE mass obtained (g), m_{LTW} is the initial mass of LTW (g) and F_p is the FAEE purity obtained from equation (1).

2.5. Design of experiment and determination of optimum point using RSM

The statistical analysis using the combination of RSM and MLFD as the design of experiment (DOE) was performed for the determination of the optimum transesterification parameters to obtain the maximum

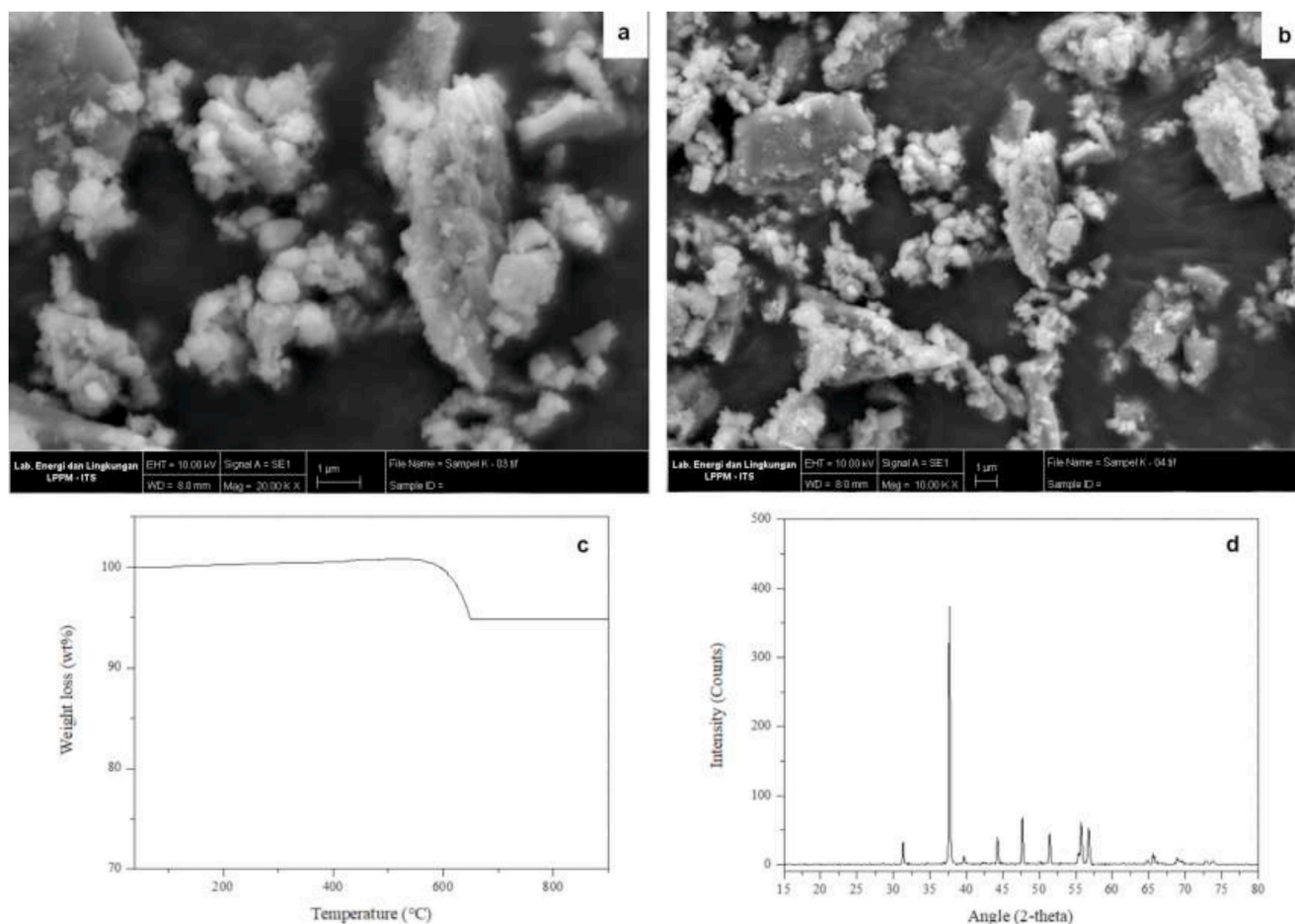


Fig. 1. (a)–(b) FESEM images, (c) TGA analysis, (d) XRD pattern of CS-based CaO.

Table 3

The textural properties of CS and CS-based CaO.

Materials	Specific surface area (S_{BET} , m^2/g)	Pore volume (V_p , cm^3/g)
CS	0.91	0.022
CS-based CaO	12.47	0.081

yield of FAEE as the response. The input variables, namely m_c (wt%), t (h), and m_{e0} (mol/mol) were chosen as the critical parameters due to their relevance to the industrial applicability since these parameters greatly affect the processing efficiency and operational cost. While both t and m_{e0} are separated into three levels: low (1), middle (2), and high (3), m_c is classified into five levels with an ascending order to accurately observe the influence of the parameter on the yield of FAEE (wt%). Table 1 presents the encoded parameters and their actual values.

The DOE matrix, shown in Table 2, lists the correlation between the reaction parameters for each run with their corresponding experimental and predicted responses (FAEE yield, wt%). To attain good data reproducibility and accuracy, the experimental runs were carried out in triplicates and randomized order. Analysis of variance (ANOVA) is employed by using Minitab (ver. 18.1) with a confidence level of 95% to generate the fitted equation, to describe the behavior of the three operating variables on the yield of FAEE. The goodness-of-fit analysis on the generated mathematical model is also evaluated using the R-squared value.

The following equation (3) shows the correlation between the predicted response (FAEE yield, wt%) and the input variables, where Y_{FAEE} is the predicted FAEE yield (wt%); k_0 , k_i , k_{ii} , k_{ij} are the coefficients for

the intercept, linear, quadratic, and two-way interactions of the input variables, respectively; X_i and X_j are the encoded reaction variables (A, B, C). While the value of i lies between 1 and 3 for t and m_{e0} , it ranges from 1 to 5 for m_c .

$$Y_{FAEE} = k_0 + \sum_{i=1}^3 k_i X_i + \sum_{i=1}^3 k_{ii} X_i^2 + \sum_{i=1}^3 \sum_{j=1}^3 k_{ij} X_i X_j \quad (3)$$

3. Results and discussions

3.1. Characterization of CS-based CaO

Fig. 1 (a) and (b) present the surface topographies of CS-based CaO. It is notable that the catalyst particle is irregular in shape and has a rough surface with a honeycomb-like structure (Fig. 1 (a)). The calcination reaction at 900 °C removes a substantial amount of bound water from the catalyst pores, hence creating high porosity [11]. However, it is also evident from the FESEM images that catalyst particles are aggregated, resulting in non-uniform particle size. Valverde et al. [32] stated that the presence of carbon in the CS-based CaO will induce the formation of CO₂ during the calcination. This CO₂ gas will then react with the CaO product to produce calcium carbonate, the primary cause of particle aggregation.

The textural properties of CS and CS-based CaO analyzed by nitrogen sorption are provided in Table 3. The CS-based CaO has superior properties than those of raw CS. Yoosuk et al. [33] stated that the removal of impurities and moisture during the high-temperature calcination plays a critical role in improving the porosity and textural properties of the CS-based CaO. As the surface area and pore volume of catalyst have a

Table 4
The chemical properties of LTW.

Parameters	Result
Moisture, wt%	11.45
FFA, wt%	18.89
Total crude fat, wt%	69.66
Molecular mass, g/mol	798.5
FA composition, wt%	
C14:0	4.30
C16:0	28.70
C16:1	2.60
C17:0	0.70
C18:0	13.40
C18:1	43.50
C18:2	4.90
C18:3	1.80
C20:0	0.10

proportional influence on its catalytic activity, it is expected that CS-based CaO has a comparable, if not superior, catalytic activity compared to the existing CaO catalyst.

To demonstrate the thermal stability of the CS-based CaO, a thermogravimetric analysis (TGA) was carried out, and its profile is

presented in Fig. 1 (c). The figure shows a 5 wt% decrease when the temperature is elevated from 595 °C to 650 °C which corresponds to the evaporation of chemically-bound moisture [34], decomposition, and transition of calcite (CaCO_3) to CaO [11]. As the complete decomposition of CaCO_3 can be achieved at the temperature of around 700 °C; the selection of calcination temperature at 900 °C is deemed suitable to ensure the complete phase transition of calcite and its derivatives to CaO [34,35], which leads to the formation of a porous structure. Hu et al. [11] also reported that the catalytic activity of a catalyst escalates along with the activation [11]. The XRD image (Fig. 1 (d)) shows that the diffraction pattern of CS-based CaO follows the characteristic fingerprint of CaO (JCPDS file no. 82–1691) as the primary component and calcite (JCPDS file no. 47–1743) as the minor substance.

3.2. Transesterification parameter study

The chemical properties of LTW are presented in Table 4, with palmitic acid (C16:0), stearic acid (C18:0), and oleic acid (C18:1) as the three principal fatty acids constituting LTW. As homogenous catalysts are sensitive to FFA and impurities, the conventional conversion of LTW to FAEE requires at least a two-stage process: (1) acid-catalyzed esterification to generate FAEE from the FFA content in LTW, and (2) base-

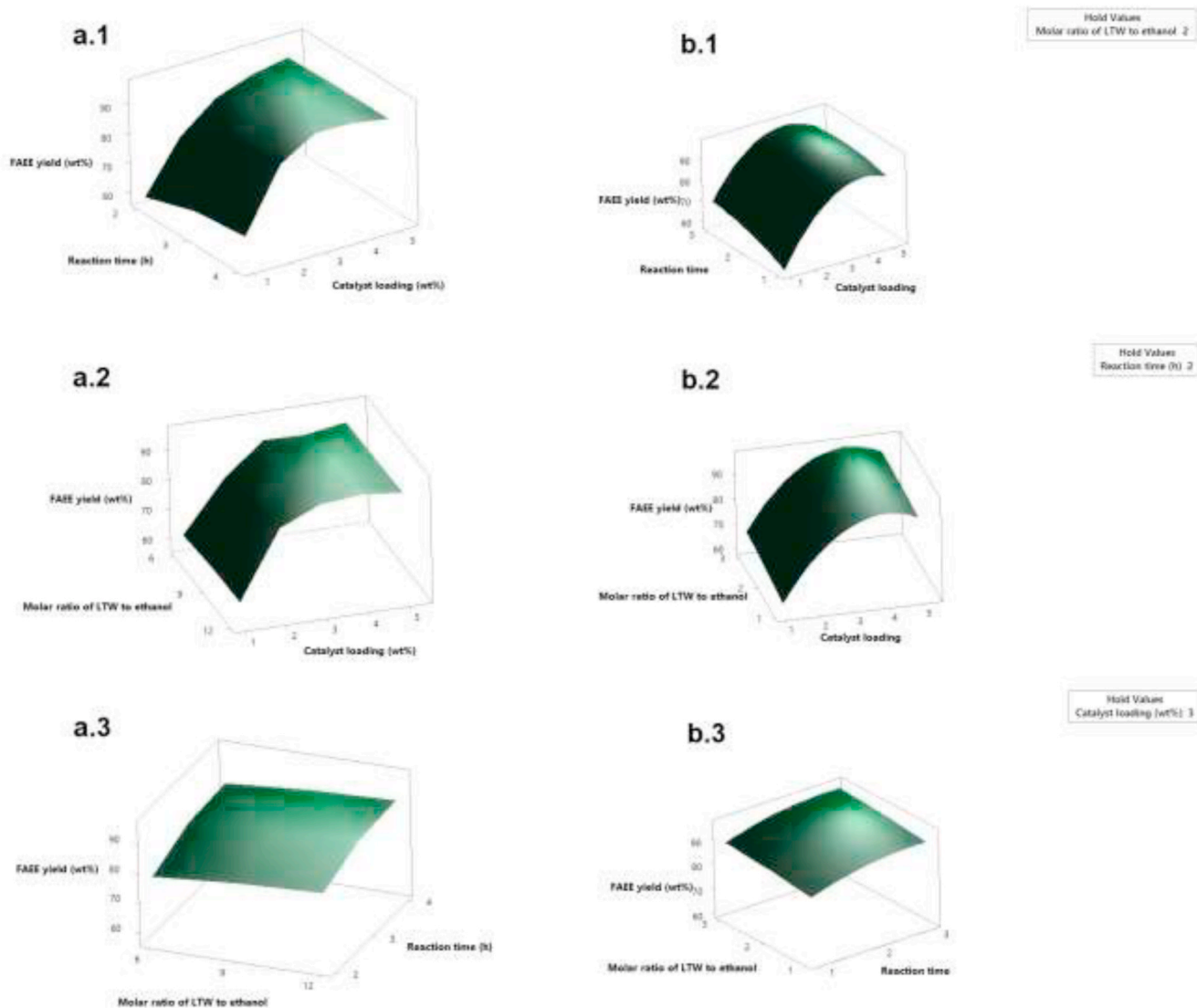


Fig. 2. (a) The experimental and (b) the predicted FAEE yield (wt%), based on their interaction between (1) catalyst loading m_c (wt%) and reaction time t (h), (2) catalyst loading m_c (wt%) and molar ratio of ethanol to LTW m_{e0} , (3) reaction time t (h) and the molar ratio of ethanol to LTW m_{e0} .

Table 5

The three-way ANOVA study of the tested variables.

Term	Coef	SE Coef	T-Value	P-Value
Constant	92.76	1.01	92.25	0.000
A	13.433	0.561	23.95	0.000
B	3.507	0.486	7.22	0.000
C	1.713	0.486	3.53	0.001
A ²	-13.432	0.948	-14.17	0.000
B ²	-2.127	0.841	-2.53	0.016
C ²	-0.347	0.841	-0.41	Non-significant
(A)(B)	-2.190	0.687	-3.19	0.003
(A)(C)	-0.613	0.687	-0.89	Non-significant
(B)(C)	-0.105	0.595	-0.18	Non-significant
R-squared (R ²)			0.9607	
Adjusted R-squared (Adj-R ²)			0.9506	
Predicted R-squared (Pred-R ²)			0.9317	

catalyzed transesterification to convert the acyl glycerides into FAEE. However, heterogeneous catalysts show good tolerance towards the FFA and water content in the lipid materials, therefore efficient conversion from LTW to FAEE can be achieved in a single step.

Fig. 2 presents the yield of FAEE obtained at various m_c , t , and m_{eo} . The experimental results indicate that the catalyst amount, specifically the number of active sites offered by CS-based CaO, is proportional to the yield of FAEE (Fig. 2 (a.1) - (a.2)). Its value increases with m_c when m_c is within 3 wt%. A stagnant FAEE yield at $m_c > 3$ wt% is monitored,

$$Y_{FAEE}(\text{FAEE yield, wt}\%) = 13.23 + 29.67(A) + 15.51(B) + 4.23(C) - 3.358(A^2) - 2.127(B^2) - 0.347(C^2) - 1.095(A)(B) - 0.307(A)(C) - 0.105(B)(C) \quad (4)$$

which is probably contributed by (1) the aggregation and inconsistent dispersity of the catalyst in the reaction system [36], and (2) the enhanced viscosity of the LTW, ethanol, and catalyst mixture [37]. Wei et al. [38] also reported that the reaction rate governing step is the sorption of reactants from the catalyst; therefore, while the number of active sites is important, further addition of catalyst higher than a certain extent does not give a significant increase of the yield of FAEE.

Fig. 2 (a.1) and (a.3) show a mild increase of the FAEE yield by

extending the duration of reaction from $t = 2$ h to $t = 4$ h. Prolonged t provides sufficient opportunities for the catalyst to be dispersed and come into proper contact with the reactants, and ensures the reaction to reach the equilibrium [21]; therefore, increasing the conversion of acyl glycerides and FFA into FAEE. From another viewpoint, lengthening the duration of the reaction also gives the catalyst enough time to adsorb the reactants and desorb the resulting product [39].

The influence of m_{eo} is depicted in Fig. 2 (a.2) - (a.3). As seen from the figure, having excess ethanol from $m_{eo} = 6:1$ to $m_{eo} = 12:1$ contributes to a slightly higher FAEE yield, and its prominence is incomparable to the effect of m_c . It is known that excess alcohol in the reaction system triggers intensive contact between reactants and catalysts, hence, accelerating the reaction rate. However, this is only beneficial to a certain degree because the excess alcohol hinders the phase separation and decreases the apparent FAEE yield [40].

3.3. Process optimization

To determine the optimum operating condition, RSM combined with MLFD is statistically employed by simultaneously integrating three critical parameters (m_c , t , m_{eo}). Table 2 presents the relation between the responses and their corresponding input variables. Using the least square analysis, the experimental responses are found to fit into a second-order polynomial model as follows:

where Y_{FAEE} is the predicted FAEE yield (wt%) which is presented in Table 2; A , B , C are the coded level of reaction variables (1, 2, 3, 4, 5 for A and 1, 2, 3 for B and C). The mathematical equation indicates that all linear variables (A , B , C) give a favorable effect on the yield of biodiesel, and conversely, the other variables (A^2 , B^2 , C^2 , $(A)(B)$, $(A)(C)$, $(B)(C)$) reduce the response. The statistical ANOVA results presented in Table 5 shows that all terms, except that of C^2 , $(A)(C)$, and $(B)(C)$, are prominent to the reaction (p -value < 0.05), with the significance order of $A > A^2 >$

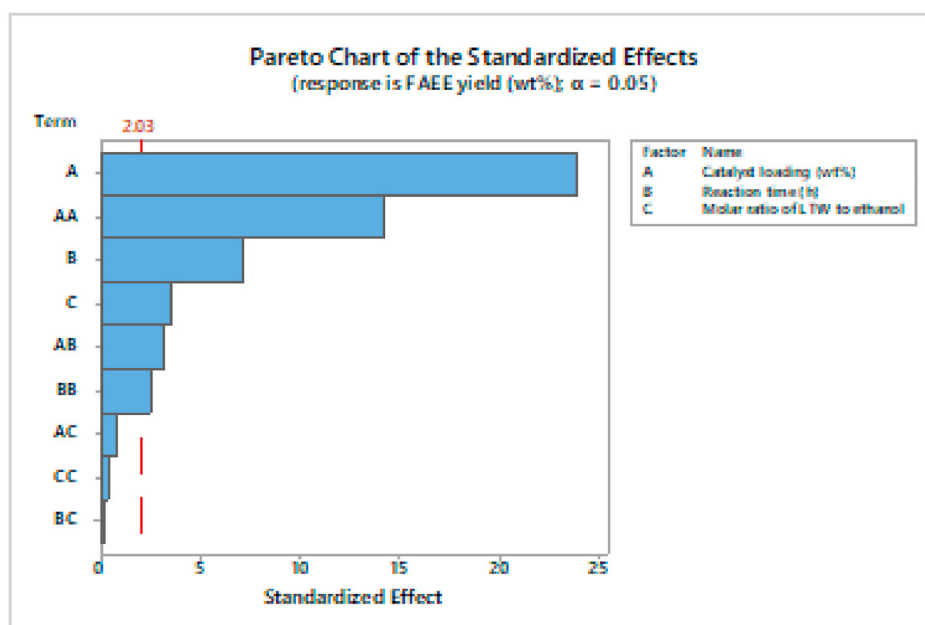


Fig. 3. The Pareto chart of the standardized effect showing the significance order of various reaction variables.

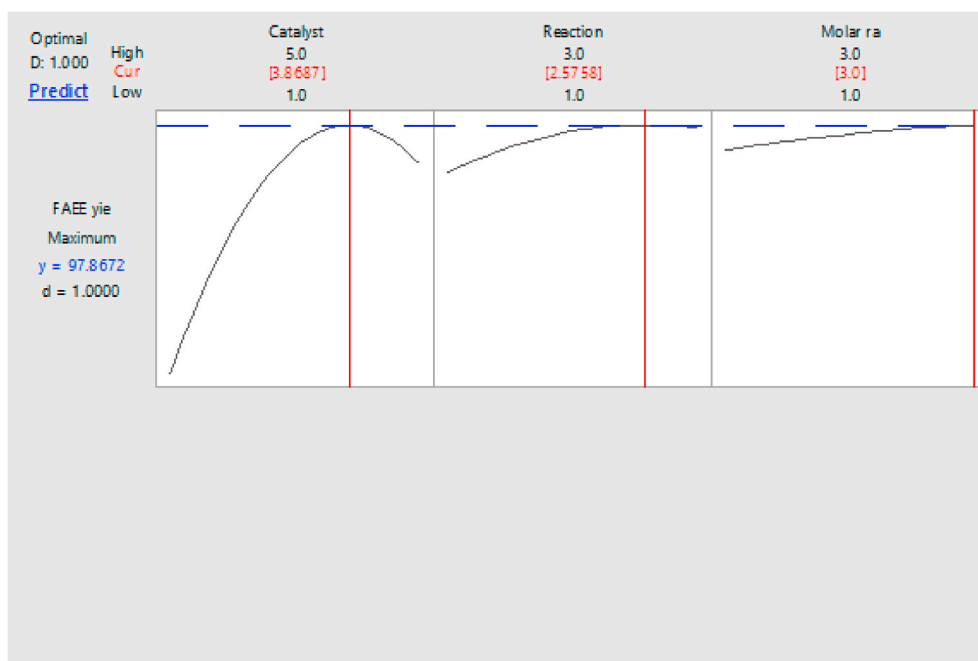


Fig. 4. The optimization plot of the reaction variables.

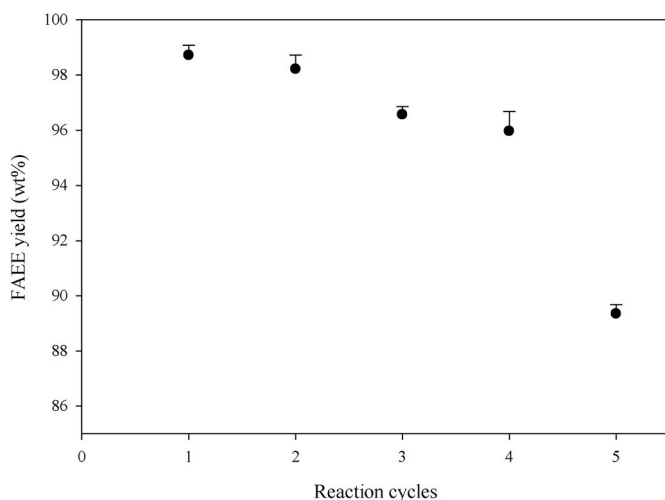


Fig. 5. The catalytic activity of reused CS-based CaO.

$B > C > (A)(B) > B^2$ as shown in Fig. 3.

The goodness-of-fit analysis for the fitted equation (equation (4)) is measured by using the R-squared (R^2), where the R^2 value for the model is obtained at 0.9607, pointing that 96.07% of the actual experimental data can be interpreted by equation (4). The values of the adjusted and predicted R^2 are also respectively monitored at 0.9506 and 0.9317, indicating that the predicted and experimental FAEE yields are in good agreement. Table 2 shows that the average standard error of estimate (SEE) between the two corresponding responses is observed at 1.24% ($n = 45$), indicating sufficient data accuracy. Fig. 2 (b.1) – (b.3) further prove that both experimental and predicted plots share a similar response profile. Therefore, the mathematical model is considered adequate to predict the response for all input variables within the tested range.

The optimized reaction condition is generated using Minitab (ver. 18.1) and predicted at $m_c = 3.87$ wt%, $t = 3.58$ h, and $m_{eo} = 12:1$. The computed response at this condition is obtained at 97.9 wt%, with desirability = 1.0 (Fig. 4). To confirm the plausibility of the mathematical model, triplicate experiments are carried out at the optimum condition. The average FAEE yield is found at 98.7 ± 0.4 wt%, with the purity of 98.6 ± 0.4 wt%. The established model is deemed reliable and accurate for all operating conditions within the tested range, as the error between the predicted and experimental results is only 0.85%. A

Table 6

The performance of various techniques for the production of biodiesel from waste-originated materials.

Lipid material	Catalyst type	Operating condition	Biodiesel yield (wt %)	Catalyst reusability	Reference
Vegetable oil wastewater sludge	N/A (Subcritical methanol)	$T = 215$ °C, $P = 6.5$ MPa, $m_{mo}^b = 5:1$, $t = 12$ h	92.7	-	[41]
Waste cooking oil	Zn-doped waste-egg shells CaO	$T = 65$ °C, $m_c = 5$ wt%, $m_{mo}^b = 20:1$, $t = 4$ h	96.7	2	[42]
Tallow fats	KOH	$T = 60$ °C, $m_c = 0.8$ wt%, $m_{mo}^b = 6:1$, $t = 2$ h	90.8	-	[43]
LTW	N/A ^a (Supercritical ethanol)	$T = 374.6$ °C, $P = 15$ MPa, $m_{eo} = 40.02:1$, $t = 47.4$ min	98.9	-	[16]
LTW	CS-based CaO	$T = 60$ °C, $m_c = 3.87$ wt%, $m_{eo} = 12:1$, $t = 3.58$ h	98.7	4	This work

^a Not available.

^b m_{mo} stands for molar ratio of methanol to oil.

Table 7
The properties of LTW-based biodiesel.

Properties	Methods	LTW-based biodiesel	ASTM D6751	Diesel fuel (ASTM D975-08)
Kinematic viscosity (at 40 °C), mm ² /s	ASTM D445	2.1	1.9–6.0	1D: 1.3–2.4 2D: 1.9–4.1
Density (at 15 °C, kg/m ³)	ASTM D1298	865	-	-
Flash point, °C	ASTM D93	167	93 min	1D: 38 min 2D: 52 min
Cloud point	ASTM D2500	10.2	-	-
Cetane number	ASTM D613	53	47 min	46 min
Water and sediment, vol%	ASTM D2709	0.01	0.05 max	0.05 max
Acid value, mg KOH/g	ASTM D664	0.22	0.50 max	-
Iodine value, g I ₂ /100 g	AOCS Cd 1-25	52.9	-	-
Ester content, wt%	EN 14103	98.7	-	-
Linolenic acid ethyl ester content, wt%	EN 14103	1.2	-	-
Polyunsaturated ethyl ester content, wt%	EN 15779	6.1	-	-
Total glycerine, wt%	ASTM D6584	0.16	0.24 max	-
Free glycerine, wt%	ASTM D6584	0.01	0.02 max	-
Sulfur, ppm	ASTM D5453	3.67	15 max (S15) 500 max (S500)	1D and 2D: 15 max (S15) 500 max (S500)
Phosphorus, ppm	ASTM D4951	0.21	10 max	-
Carbon residue, wt%	ASTM D4530	0.002	0.05 max	1D: 0.15 max 2D: 0.35 max
Oxidation stability, h	EN 14112	12.7	3 min	-
Calorific value, MJ/kg	ASTM D240	44.67	-	-

relatively short reaction time ($t = 3.58$ h) and low catalyst amount ($m_c = 3.87$ wt%) is highly beneficial in practice, as these variables directly influence the production efficiency.

The reusability of CS-based CaO is presented in Fig. 5, where the results show that the regenerated CS-based CaO can maintain a high yield of FAEE (>90 wt%) until the fourth run before significantly decline to 89.4 wt% in the fifth cycle. The FAEE yields for the first four cycles are 98.7 wt%, 98.2 wt%, 96.6 wt%, 96.0 wt%, with the respective purity of 98.6 wt%, 98.9 wt%, 97.3 wt, 98.2 wt%. The deactivation of CS-based CaO is probably due to the clogged pores, caused by the deposition of deactivation-induced molecules, e.g., free glycerol, acyl glycerides, and biodiesel. The FFA content may as well deactivate the basic sites of CS-based CaO through neutralization [5] to form calcium carboxylate. A comparative study of the biodiesel production from waste-originated materials using various methods is presented in Table 6. In general, the conversion of LTW to biodiesel using CS-based CaO shows comparable performance with the other preparation processes, indicated by its high product yield (higher than 90 wt%) and reusability number.

3.4. Characteristics of LTW-based biodiesel

Table 7 presents the fuel properties of LTW-based biodiesel generated using CS-based CaO as a catalyst. The measurements indicate that the properties of the resulting biodiesel product are in accordance with the standard of ASTM D6751 and ASTM D975-08. A high flash point, which is the result of the sufficient post-separation step, shows that the product can be treated, stored, and transported safely. Its calorific value, 44.67 MJ/kg, is within the range of that of petroleum diesel fuel (42–46

MJ/kg) [44]. The chemical compositional analysis of the LTW-based FAEE using GC-FID shows that there are ten distinguished peaks in the chromatogram: myristic acid ethyl ester (C14:0), myristoleic acid ethyl ester (C14:1), palmitic acid ethyl ester (C16:0), palmitoleic acid ethyl ester (C16:1), heptadecanoic acid ethyl ester (C17:0), stearic acid ethyl ester (C18:0), oleic acid ethyl ester (C18:1), linoleic acid ethyl ester (C18:2), α -linolenic acid ethyl ester (C18:3), arachidic acid ethyl ester (C20:0).

4. Conclusions

Successful conversion of LTW to biodiesel is achieved using a CS-based CaO, with the highest FAEE yield of 98.7 ± 0.4 wt% (purity of 98.6 ± 0.4 wt%) obtained at the following reaction condition: $m_c = 3.87$ wt%, $t = 3.58$ h, and $m_{eo} = 12:1$. The CS-based CaO shows good reusability; the FAEE yield stays above 90 wt% for four reaction cycles. The fuel properties of LTW-based FAEE comply with ASTM D6751 and ASTM D975-08. The valorization of CS and LTW will prominently allow better environmental destination for these wastes and meanwhile offers an environmentally benign route to produce high value-added renewable energy.

Acknowledgment

This research did not receive any specific grant from funding agencies in the public, commercial, or not-for-profit sectors.

References

- [1] Y. Widria, Prospek Pasar Ekspor Rajungan Dan Kepiting Indonesia Ke China [The Prospect of Indonesian Crab and Crab Export Market to China], Balai Besar Pengujian, Penerapan Prod. Kelaut. Dan Perikan., 2019 accessed, <https://kcp.go.id/djpdspkp/bbp2hp/artikel/15122-prospek-pasar-ekspor-rajungan-dan-kepiting-indonesia-ke-china>. (Accessed 15 September 2020).
- [2] N. Yan, X. Chen, Don't waste seafood waste: turning cast-off shells into nitrogen-rich chemicals would benefit economies and the environment, *Nature* 524 (2015) 155–157.
- [3] P.L. Boey, G.P. Maniam, S.A. Hamid, Performance of calcium oxide as a heterogeneous catalyst in biodiesel production: a review, *Chem. Eng. J.* 168 (2011) 15–22, <https://doi.org/10.1016/j.cej.2011.01.009>.
- [4] W. Roschat, T. Siritanon, B. Yoosuk, V. Promarak, Biodiesel production from palm oil using hydrated lime-derived CaO as a low-cost basic heterogeneous catalyst, *Energy Convers. Manag.* 108 (2016) 459–467, <https://doi.org/10.1016/j.enconman.2015.11.036>.
- [5] M. Kouzu, J.S. Hidaka, Transesterification of vegetable oil into biodiesel catalyzed by CaO: a review, *Fuel* 93 (2012) 1–12, <https://doi.org/10.1016/j.fuel.2011.09.015>.
- [6] D.M. Marinković, M.V. Stanković, A.V. Veličković, J.M. Avramović, M. R. Miladinović, O.O. Stamenković, V.B. Veljković, D.M. Jovanović, Calcium oxide as a promising heterogeneous catalyst for biodiesel production: current state and perspectives, *Renew. Sustain. Energy Rev.* 56 (2016) 1387–1408, <https://doi.org/10.1016/j.rser.2015.12.007>.
- [7] I.M. Rizwanul Fattah, H.C. Ong, T.M.I. Mahlia, M. Mofijur, A.S. Silitonga, S. M. Ashrafur Rahman, A. Ahmad, State of the art of catalysts for biodiesel production, *Front. Energy Res.* 8 (2020) 1–17, <https://doi.org/10.3389/fenrg.2020.00101>.
- [8] W. Suryaputra, I. Winata, N. Indraswati, S. Ismadji, Waste capiz (Amusium cristatum) shell as a new heterogeneous catalyst for biodiesel production, *Renew. Energy* 50 (2013) 795–799, <https://doi.org/10.1016/j.renene.2012.08.060>.
- [9] M. Yuliana, S.P. Santoso, F.E. Soetaredjo, S. Ismadji, A.E. Angkawijaya, W. Irawaty, Y.-H. Ju, P.L. Tran-Nguyen, S.B. Hartono, Utilization of waste capiz shell – based catalyst for the conversion of leather tanning waste into biodiesel, *Int. J. Chem. Environ. Eng.* 8 (2020) 104012, <https://doi.org/10.1016/j.jece.2020.104012>.
- [10] C. Chambers, A. Holliday, Acids and bases: oxidation and reduction. *Mod. Inorg. Chem., Butterworth & Co., Chichester*, 1975, pp. 84–111.
- [11] S. Hu, Y. Wang, H. Han, Utilization of waste freshwater mussel shell as an economic catalyst for biodiesel production, *Biomass Bioenergy* 35 (2011) 3627–3635, <https://doi.org/10.1016/j.biombioe.2011.05.009>.
- [12] A. Buasri, N. Chaiyut, V. Loryuenyong, P. Worawanitchaphong, S. Trongyong, Calcium oxide derived from waste shells of mussel, cockle, and scallop as the heterogeneous catalyst for biodiesel production, *Sci. World J.* 2013 (2013), <https://doi.org/10.1155/2013/460923>.
- [13] S. Niju, M.M.M.S. Begum, N. Anantharaman, Modification of egg shell and its application in biodiesel production, *J. Saudi Chem. Soc.* 18 (2014) 702–706, <https://doi.org/10.1016/j.jscs.2014.02.010>.
- [14] Y.Y. Margaretha, H.S. Prastyo, A. Ayucitra, S. Ismadji, Calcium oxide from pomacea sp. shell as a catalyst for biodiesel production, *Int. J. Energy Environ. Eng.* 3 (2012) 1–9, <https://doi.org/10.1186/2251-6832-3-33>.

- [15] S. Kaewdaeng, P. Sintuya, R. Nirunsin, Biodiesel production using calcium oxide from river snail shell ash as catalyst, *Energy Procedia* 138 (2017) 937–942, <https://doi.org/10.1016/j.egypro.2017.10.057>.
- [16] M. Yuliana, S.P. Santoso, F.E. Soetaredjo, S. Ismadji, A. Ayucitra, A. E. Angkawijaya, Y.-H. Ju, P.L. Tran-Nguyen, A One-Pot Synthesis of Biodiesel from Leather Tanning Waste Using Supercritical Ethanol: Process Optimization, *Biomass Bioenergy* vol. 142 (2020), <https://doi.org/10.1016/j.biombioe.2020.105761>.
- [17] J. Kanagaraj, K.C. Velappan, N.K. Chandra Babu, S. Sadulla, Solid wastes generation in the leather industry and its utilization for cleaner environment - a review, *J. Sci. Ind. Res. (India)* 65 (2006) 541–548, <https://doi.org/10.1002/chin.200649273>.
- [18] S. Zafar, Wastes generation in tanneries, *Bioenergy Consult* (2019). <https://www.bioenergyconsult.com/waste-from-tanneries/>.
- [19] F. Alihniar, *Di Industri Penyamakan Kulit Leather Tanning Industry*, 2011.
- [20] L.K. Ong, A. Kurniawan, A.C. Suwandi, C.X. Lin, X.S. Zhao, S. Ismadji, Transesterification of leather tanning waste to biodiesel at supercritical condition: kinetics and thermodynamics studies, *J. Supercrit. Fluids* 75 (2013) 11–20, <https://doi.org/10.1016/j.supflu.2012.12.018>.
- [21] V.K. Booramurthy, R. Kasimani, D. Subramanian, S. Pandian, Production of biodiesel from tannery waste using a stable and recyclable nano-catalyst: an optimization and kinetic study, *Fuel* 260 (2020) 116373, <https://doi.org/10.1016/j.fuel.2019.116373>.
- [22] S. Krishnan, Z.A. Wahid, L. Singh, M. Sakinah, Production of biodiesel using tannery fleshing as a feedstock: an investigation of feedstock pre-treatment via solid-state fermentation, *ARNP J. Eng. Appl. Sci.* 11 (2016) 7354–7357.
- [23] S. Çolak, G. Zengin, H. Özgünay, Ö. Sari, H. Sarikahya, L. Yüceer, Utilization of leather industry pre-fleshings in biodiesel production, *J. Am. Leather Chem. Assoc.* 100 (2005) 137–141.
- [24] H. Dagne, R. Karthikeyan, S. Feleke, Waste to energy: response surface methodology for optimization of biodiesel production from leather fleshing waste, *J. Energy* (2019) 1–19, <https://doi.org/10.1155/2019/7329269>.
- [25] Ş. Altun, F. Yaşar, Biodiesel production from leather industry wastes as an alternative feedstock and its use in diesel engines, *Energy Explor. Exploit.* 31 (2013) 759–770, <https://doi.org/10.1260/0144-5987.31.5.759>.
- [26] J. Pecha, K. Kolomaznik, M. Barinova, L. Sanek, High quality biodiesel and glycerin from fleshings, *J. Am. Leather Chem. Assoc.* 107 (2012) 312–322.
- [27] B. Panneton, H. Phillion, P. Dutilleul, R. Thériault, M. Khelifi, Full factorial design versus centra composite design: statistical comparison and implications for spray droplet deposition, *experiments* 42 (1999) 877–883.
- [28] J. Cutting, Research methods in psychology (Lectures Week 7), (n.d.), <https://psychology.illinoisstate.edu/jccutti/psych231/SP01/wk7/week7.htm>. (Accessed 5 May 2021). accessed.
- [29] P. Verma, M.P. Sharma, Comparative analysis of effect of methanol and ethanol on Karanja biodiesel production and its optimisation, *Fuel* 180 (2016) 164–174, <https://doi.org/10.1016/j.fuel.2016.04.035>.
- [30] Basque Research, Ethanol and Heterogeneous Catalysts for Biodiesel Production, Sciencedaily, 2014. www.sciencedaily.com/releases/2014/11/141112084246.htm.
- [31] F.H. Santosa, L. Laysandra, F.E. Soetaredjo, S.P. Santoso, S. Ismadji, M. Yuliana, A facile noncatalytic methyl ester production from waste chicken tallow using single step subcritical methanol: optimization study, *Int. J. Energy Res.* 43 (2019) 8852–8863, <https://doi.org/10.1002/er.4844>.
- [32] J.M. Valverde, P.E. Sanchez-Jimenez, L.A. Perez-Maqueda, Limestone calcination nearby equilibrium: kinetics, CaO crystal structure, sintering and reactivity, *J. Phys. Chem. C* 119 (2015) 1623–1641, <https://doi.org/10.1021/jp508745u>.
- [33] B. Yoosuk, P. Udomsap, B. Puttasawat, P. Krasae, Improving transesterification activity of CaO with hydration technique, *Bioresour. Technol.* 101 (2010) 3784–3786, <https://doi.org/10.1016/j.biortech.2009.12.114>.
- [34] Z.X. Tang, Z. Yu, Z.L. Zhang, X.Y. Zhang, Q.Q. Pan, L.E. Shi, Sonication-assisted preparation of CaO nanoparticles for antibacterial agents, *Quim. Nova* 36 (2013) 933–936, <https://doi.org/10.1590/S0100-40422013000700002>.
- [35] Y. Zhu, S. Wu, X. Wang, Nano CaO grain characteristics and growth model under calcination, *Chem. Eng. J.* 175 (2011) 512–518, <https://doi.org/10.1016/j.cej.2011.09.084>.
- [36] C. Samart, C. Chaia, P. Reubroycharoen, Biodiesel production by methanolysis of soybean oil using calcium supported on mesoporous silica catalyst, *Energy Convers. Manag.* 51 (2010) 1428–1431, <https://doi.org/10.1016/j.enconman.2010.01.017>.
- [37] B. Gurunathan, A. Ravi, Biodiesel production from waste cooking oil using copper doped zinc oxide nanocomposite as heterogeneous catalyst, *Bioresour. Technol.* 188 (2015) 124–127, <https://doi.org/10.1016/j.biortech.2015.01.012>.
- [38] Z. Wei, C. Xu, B. Li, Application of waste eggshell as low-cost solid catalyst for biodiesel production, *Bioresour. Technol.* 100 (2009) 2883–2885, <https://doi.org/10.1016/j.biortech.2008.12.039>.
- [39] T. Pangestu, Y. Kurniawan, F.E. Soetaredjo, S.P. Santoso, W. Irawaty, M. Yuliana, S. B. Hartono, S. Ismadji, The synthesis of biodiesel using copper based metal-organic framework as a catalyst, *J. Environ. Chem. Eng.* 7 (2019) 103277, <https://doi.org/10.1016/j.jece.2019.103277>.
- [40] G. Anastopoulos, Y. Zannikou, S. Stourmas, S. Kalligeros, Transesterification of vegetable oils with ethanol and characterization of the key fuel properties of ethyl esters, *Energies* 2 (2009) 362–376, <https://doi.org/10.3390/en20200362>.
- [41] F. Gunawan, A. Kurniawan, I. Gunawan, Y.H. Ju, A. Ayucitra, F.E. Soetaredjo, S. Ismadji, Synthesis of biodiesel from vegetable oils wastewater sludge by in-situ subcritical methanol transesterification: process evaluation and optimization, *Biomass Bioenergy* 69 (2014) 28–38, <https://doi.org/10.1016/j.biombioe.2014.07.005>.
- [42] M.J. Borah, A. Das, V. Das, N. Bhuyan, D. Deka, Transesterification of waste cooking oil for biodiesel production catalyzed by Zn substituted waste egg shell derived CaO nanocatalyst, *Fuel* 242 (2019) 345–354, <https://doi.org/10.1016/j.fuel.2019.01.060>.
- [43] T.M. Mata, N. Cardoso, M. Ornelas, S. Neves, N.S. Caetano, Sustainable production of biodiesel from tallow, lard and poultry fat and its quality evaluation, *Chem. Eng. Trans.* 19 (2010) 13–18, <https://doi.org/10.3303/CET1019003>.
- [44] W.N. Association, Heat values of various fuels. <http://www.world-nuclear.org/information-library/facts-and-figures/heat-values-of-various-fuels.aspx>, 2018.